A comparative study of the harmonic balance method and the orthogonal collocation method on stiff non linear systems

Sami Karkar[a,b], Bruno Cochelin[a], Christophe Vergez[a]

[a] *LMA, CNRS UPR 7051, Centrale Marseille, F-13402 Marseille cedex 20, FRANCE*
[b] *Currently at: LEMA, EPFL, Station 11, CH-1015 Lausanne, SWITZERLAND*

Abstract

The high-order purely frequency-based Harmonic Balance Method (HBM) presented by Cochelin and Vergez [1] and extended by Karkar et al. [2] now allows to follow the periodic solutions of regularized non-smooth systems (stiff systems). This paper compares its convergence property to a reference method in applied mathematics: orthogonal collocation with piecewise polynomials. A first test is conducted on a nonlinear smooth 2 degree-of-freedom spring mass system, showing better convergence of the HBM. The second test is conducted on a one degree-of-freedom vibro-impact system with a very stiff regularization of the impact law. The HBM continuation of the nonlinear mode was found to be very robust, even with a very large number of harmonics. Surprisingly, the convergence was again found to be better than the one of the collocation method for this vibro-impact system.

Keywords: nonlinear dynamical systems, periodic solutions, asymptotic numerical method, harmonic balance, orthogonal collocation

Email addresses: sami.karkar@epfl.ch (Sami Karkar), bruno.cochelin@centrale-marseille.fr (Bruno Cochelin), vergez@lma.cnrs-mrs.fr (Christophe Vergez)

1. Introduction

The literature is crudely lacking comparative studies between purely time-based and purely frequency-based numerical methods for computing periodic solutions of nonlinear dynamical systems. This is especially true regarding the behavior of numerical methods when addressing stiff mechanical systems like impacting oscillators (vibro-impact system). This paper aims at comparing two such methods, in a general framework where one wishes to compute families, or branches, of periodic solutions of such systems using a numerical continuation algorithm. This is an important issue in many scientific fields and engineering applications.

In literature, various numerical methods have been proposed to directly compute such periodic solutions [3–6] without resorting to numerical time integration techniques, which provide stable periodic solutions only as a limit set and can be very time-consuming, especially for stiff systems. These direct numerical methods are generally classified into two main categories referred to as the frequency domain approach and the time domain approach.

The emblematic method for the frequency domain approach is the so-called harmonic balance method (HBM) which relies on the representation of the periodic orbit by a truncated Fourier series for the unknown state variables. The HBM substitutes the series into the nonlinear governing equation, collecting terms with the same harmonic number and dropping terms with harmonic numbers not in the Fourier series. This leads to solving an algebraic system for the Fourier coefficients which balances harmonics. HBM is better presented as a weighted residual method: it is a Galerkin method with Fourier basis and Fourier test functions, and for which convergence has been established for instance by Urabe [7]. Note that some authors describe the HBM as unpractical or cumbersome, as it implies analytical derivation

of the relations between Fourier coefficients involved in the nonlinear terms. However, previous works have shown that: first, most nonlinearities can be recast as quadratic polynomials using additional variables; and second, in the quadratic case it is very easy to automate this analytical work (see [2]). Many variations of the basic HBM exist, such as the Alternating Frequency Time-HBM [8], the Multi-HBM [9], the Incremental HBM [10], the Adaptive HBM [11]. Some of these variations improve usability, performance, or robustness. Some adapt to situations such as non-smooth systems [12] or delay systems for example.

Two emblematic methods for the time domain approach are the shooting method [4, 5] (not considered here, as it does use time integration) and the global finding of periodic orbits using a boundary value approach [6]. The orthogonal collocation with piecewise polynomials (later referred to as collocation) belongs to the second one: the periodic orbit is divided into mesh intervals, the unknown state variables are represented by polynomials on each interval and the governing equations are collocated at Gauss points. This collocation method may also be seen as a weighted residual method (in this case, a Petrov-Galerkin method) with piecewise polynomial basis and Dirac test functions, and many variations exist. To end, it is worth noting note that a third category could have been introduced for trigonometric collocation methods [13], or similarly the High-Dimensional HBM [14] which, despite the name, is more a collocation method than an HBM as shown by [15]. Methods belonging to the latest category are once more weighted residual methods, but with Fourier basis and Dirac test function.

Today, HBM is very popular in electrical engineering (electronic circuit) and in mechanical engineering (structural dynamics, rotor dynamics) while the collocation method is very popular for biological systems, population sys-

tems, chemical reactions analysis and more generally for applied mathematics (the collocation method is for instance implemented in the AUTO software [16], as well as in the MATCONT package [17], a MATLAB [18] toolbox). So, it seems that the choice between the frequency domain approach and the time domain approach is not only a question of performance and ease of implementation, but also a question of experience inside a scientific field. As stated earlier, the literature lacks comparisons between these two categories of methods: typical papers describe a numerical method and demonstrate its performance on selected representative examples, but comparisons are seldom performed.

The present study compares the high-order purely frequency HBM presented in [1] and extended in [2], with the piecewise polynomial collocation method. For this, a still challenging mechanical problem is chosen: periodic solutions continuation of a regularized vibro-impact system, that is, nonlinear mode calculations of a non-smooth system. The comparison is carried out using the asymptotic numerical method (ANM) for the continuation and each of the aforementioned methods for the discretization. Because many variations exist for each category of methods, a few conditions have to be fixed for the comparison. Hereafter, focus is brought to the accuracy of the solution versus the number of unknowns in the algebraic system. Second, the comparison is limited to small size dynamical systems. Third, no adaptive mesh is used for the collocation and no harmonic selection is used for the HBM. Within this framework, and despite the common wisdom that would advise against using the HBM for systems with stiff nonlinearities, the HBM achieves a better convergence rate than the collocation, even for very stiff problem.

The paper is organized as follows: in section 2, the harmonic balance method and the orthogonal collocation with piecewise polynomials method are reviewed, and their theoretical convergence rates are recalled. In section 3, their convergences are compared on a toy-model composed of a slightly nonlinear, one-mass, two-spring plane system (representative of shells under large strain), as well as their efficiency for calculating periodic orbit families, when coupled with the ANM continuation technique. Then, in section 4, the same methodology is used to compare both approaches on a highly nonlinear system: an impacting oscillator with exponential restoration force. The conclusions of this comparative study are outlined in the last section.

2. Discretization methods for periodic orbits

In this section, the two methods that are used here for solving the periodic boundary-value problem that consists in finding a periodic solution of a given autonomous, nonlinear dynamical system are briefly reviewed. The problem is to find $\mathbf{Y} : \mathbb{R} \to \mathbb{R}^n$ and its associated period $T \in \mathbb{R}_+$ such that $\forall t \in \mathbb{R}$,

$$\mathbf{Y}'(t) = f(\mathbf{Y}(t)) \tag{1}$$

$$\mathbf{Y}(t) = \mathbf{Y}(t+T) \tag{2}$$

where f is a nonlinear application $\mathbb{R}^n \to \mathbb{R}^n$ and the prime sign denotes the time derivative.

The general principle of a spectral method is to choose a vector-space $\mathbb{E}$ in which one wishes to approximate the solutions, together with a basis of this space: the representation functions $\{\phi_i(t)\}$. Then one writes a number of algebraic equations resulting from the orthogonalization of the residue $\mathcal{R}(\mathbf{Y}(t)) = \mathbf{Y}'(t) - f(\mathbf{Y}(t))$ to this vector-space, with respect to the corresponding scalar product. This second step is usually carried out by canceling

out the projection of the system's ordinary differential equations onto a set of functions, usually but not necessarily a basis of $\mathbb{E}$: the test (or weighting) functions. The reader is referred to Orszag [19] and Karniadakis and Sherwin [20] for the original works and a recent reformulation on spectral and pseudo-spectral methods.

2.1. The harmonic balance method

In the case of the harmonic balance method, the solution of (1–2) is approximated with a truncated Fourier series:

$$\hat{\mathbf{Y}}(t) = \mathbf{Y}_0 + \sum_{k=1}^{H} \mathbf{Y}_{2k-1} \cos(k\omega t) + \mathbf{Y}_{2k} \sin(k\omega t)$$

the vector-space of the approximation being spanned by the functions:
$\{1, \cos(\omega t), \sin(\omega t), \ldots, \cos(H\omega t), \sin(H\omega t)\}$,
where $\omega = 2\pi/T$ is the angular frequency of the solution and H the chosen order of truncation.

The *balance* of the harmonics consists in canceling out the projection of the residue obtained with this truncated series $\mathcal{R}(\hat{\mathbf{Y}}) = \hat{\mathbf{Y}}' - f(\hat{\mathbf{Y}})$ onto each function of the basis. Thus, the test functions are identical to the representation functions. The chosen scalar product is defined as:

$$< u, v >= \frac{1}{T} \int_0^T u(t)v(t)dt \tag{3}$$

Thus comes the following $2H+1$ vector-valued, algebraic equations:

$$\begin{aligned} < \mathcal{R}(\hat{\mathbf{Y}}), 1 > &= 0 \\ < \mathcal{R}(\hat{\mathbf{Y}}), \cos(\omega t) > &= 0 \\ < \mathcal{R}(\hat{\mathbf{Y}}), \sin(\omega t) > &= 0 \\ &\vdots \\ < \mathcal{R}(\hat{\mathbf{Y}}), \cos(H\omega t) > &= 0 \\ < \mathcal{R}(\hat{\mathbf{Y}}), \sin(H\omega t) > &= 0 \end{aligned}$$

Depending on the form of f and on the number of harmonics H, and using trigonometric identities, an algebraic system is obtained. It consists of $n(2H+1)$ nonlinear, algebraic equations in the $n(2H+1)$ unknowns that composes the vector $\{\mathbf{Y}_0^t, \mathbf{Y}_1^t, \mathbf{Y}_2^t, \ldots, \mathbf{Y}_{2H-1}^t, \mathbf{Y}_{2H}^t\}^t$ (the notation $\cdot^t$ denoting transposition).

In practice, obtaining this system explicitly may be difficult. But in the case where f can be recast as a quadratic polynomial, Cochelin and Vergez [1] showed that the explicit form can be obtained automatically, and for any order of truncation H. The method has been extended to any kind of nonlinearities by Karkar et al. [2].

In the case of autonomous systems, to get a well posed problem, one additional equation is needed: when a solution of (1–2) exists, any time-shift of this solution is also a solution. The additional equation is thus known as the *phase equation*, because it is obtained by prescribing the phase of the solution. It is related both to the initial value of the solution, and to the reference used for the time variable. The phase condition may be prescribed several ways, see Doedel [6] and Seydel [5] for details.

In the case of the HBM, *one* coefficient of the Fourier series of *one* com-

ponent of $\mathbf{Y}$ may be set to 0 for the phase equation. This enables to get a well-posed algebraic system $\mathbf{R}(\mathbf{U}) = 0$ of size $n(2H+1)+1$ where the unknown vector $\mathbf{U}$ is:

$$\mathbf{U} = \left[\mathbf{Y}_0^t, \mathbf{Y}_1^t, \ldots, \mathbf{Y}_{2H}^t, \omega\right]^t.$$

2.2. Orthogonal collocation at Gauss points with piecewise polynomial

The solution of (1–2) is approximated by a continuous, periodic, piecewise polynomial of order p. The chosen collocation scheme is that described in Doedel [6], as used in the AUTO software [16], except for the mesh that is not adaptive in our implementation.

First, the period $[0, T]$ is divided into a set of N subintervals $[t_j, t_{j+1}]$, where $h = t_{j+1} - t_j$ is the size of the subintervals, $t_0 = 0$ and $t_N = T$.

Then, on each subinterval, the solution is locally sampled in $p+1$ equidistant points, including the subinterval borders:

$$\mathbf{Y}_{j,i} = \mathbf{Y}(t_{j,i}) = \mathbf{Y}(t_j + \frac{i}{p}h), \qquad i \in [0..p] \tag{4}$$

and interpolated on that interval using the Lagrange polynomials of order p, $\{\ell_{j,i}\}$, based on the $p+1$ sampling instants $t_{j,i}$:

$$\forall t \in [t_j, t_{j+1}], \qquad \hat{\mathbf{Y}}(t) = \sum_{i=0}^{p} \mathbf{Y}_{j,i}\ell_{j,i}(t) \tag{5}$$

The set of representation functions is obtained by extension of the definition domain of each local Lagrange polynomial $\ell_{j,i}$ to $[0, T]$, setting its value to zero outside of its initial definition domain $[t_j, t_{j+1}]$. Thus, the approximation of the solution is written:

$$\hat{\mathbf{Y}}(t) = \sum_{j=0}^{N-1}\sum_{i=0}^{p} \mathbf{Y}_{j,i}\ell_{j,i}(t).$$

The continuity constraint is imposed by adding the equations $\mathbf{Y}_{j,p} = \mathbf{Y}_{j+1,0}$ for $j = 0..N-1$, or simply by using the same variable for both vector of each pair.

Here, the test functions are Dirac distributions, centered on each of the p collocation points of each of the N subintervals: $\delta(t - z_{j,i})$. The p collocation points of the j-th subinterval $z_{j,i}$ are the Gauss-Legendre points of order p, defined as the zeros of the Legendre polynomial of order p on this subinterval.

For instance, assuming $p = 3$, the zeros of the third order Legendre polynomial on its standard interval of definition $[-1, 1]$ are located at: $-\sqrt{\frac{3}{5}}, 0, \sqrt{\frac{3}{5}}$. A translation and a scaling factor is applied in order to get the position of the $\{z_{j,i}\}_{j=0..N-1,\, i=1..p}$ relative to the full period $[0, T]$.

It is convenient to keep p constant, because if its value were to be modified, the collocation points positions would need to be computed (at least on $[-1, 1]$) for every new value. Moreover, preliminary investigations using the AUTO software with a fixed mesh showed that, for non-smooth or very stiff systems, increasing the order of polynomials p is more costly and less efficient than increasing the number of elements N. This needs to be investigated in future works as the AUTO software restricts the values of p to low integers ($p \leq 7$).

Thus, in what follows, the value $p = 3$ is used. Only the h-refinement will be considered, that is increasing N.

To apply the Petrov-Galerkin method, the residue $\mathcal{R}(\hat{\mathbf{Y}}(t))$ is projected on every test function and this projection is set to zero. It follows:

$$< \mathcal{R}(\hat{\mathbf{Y}}(t)), \delta(t - z_{j,i}) >= 0 \qquad i = 1..p, j = 0..N-1 \tag{6}$$

which reduces to the *collocation* equations:

$$\mathcal{R}(\hat{\mathbf{Y}}(z_{j,i})) = 0 \qquad i = 1..p, j = 0..N-1 \tag{7}$$

These pNn algebraic equations, together with the periodicity condition $\mathbf{Y}_{0,0} = \mathbf{Y}_{N-1,p}$ (n equations) and a phase condition (one equation), form an algebraic system $\mathbf{R}(\mathbf{U}) = 0$ of size $(pN+1)n+1$ where the unknown vector $\mathbf{U}$ is:

$$\mathbf{U} = \left[\{\mathbf{Y}^t_{j,i}\}\Big|_{\substack{j=0..N-1\\ i=0..p-1}}, \mathbf{Y}^t_{N-1,p}, T\right]^t. \tag{8}$$

Recalling that $\mathbf{Y}_{j,i} = \hat{\mathbf{Y}}(t_{j,i}) \in \mathbb{R}^n$, the size of the unknown vector $\mathbf{U}$ is $(pN+1)n+1$, leading to a well posed problem.

2.3. Theoretical convergence rates

Gottlieb and Orszag [21] proved the convergence for both spectral and pseudo-spectral methods, under the assumptions of continuity and differentiability of f. The first and most important conclusion they draw is that the optimal rate of convergence highly depends on the smoothness of the solution that one tries to approximate, which itself is related to the smoothness of the function f that describes the system. De Boor and Swartz [22] further improved the p-convergence bound on the collocation method in the particular case where one uses the Gauss-Legendre points as collocating points.

In the case of a smooth solution (suppose, e.g., that f is $\mathcal{C}^\infty$), the HBM uniform convergence rate is in $\mathcal{O}(c^{-H})$ where $c \in \mathbb{R}_+$ is a constant greater than 1 and $H \in \mathbb{N}$ is the order of the approximation (the number of harmonics), whereas the orthogonal collocation at Gauss points has a uniform convergence rate in $\mathcal{O}(N^{-(p+1)})$ where $N \in \mathbb{N}$ is the number of elements in one period ($N = T/h$) and $p = 3$ is the order of the polynomial interpolation chosen for this study, which is also the number of collocation points in each subinterval.

2.4. Continuation

The computation of *families* of periodic solutions using numerical continuation assumes the dependence of $\mathbf{R}$ (that is, of f, in the first place) on an explicit parameter λ. The equation to be solved becomes: $\mathbf{Y}'(t) = f(\mathbf{Y}(t), \lambda)$. Once discretized, the system reads: $\mathbf{R}(\mathbf{U}, \lambda) = 0$. This nonlinear algebraic system of N_{tot} equations for $N_{\text{tot}} + 1$ unknowns thus possesses solutions that form a continuous[1] curve $(\mathbf{U}(\lambda), \lambda)$, known as a solution branch, that is parametrized (implicitly or explicitly) by the continuation parameter λ.

The ANM ("MAN" in French) is a powerful numerical method that allows for the computation of such branches $\mathbf{U}(\lambda)$ as high-order Taylor series in λ. The method is implemented in MANlab [23], a toolbox written for the MATLAB software [18], and both the HBM and the orthogonal collocation method are implemented on top of the continuation scheme.

The following parameters of the ANM have been used in MANlab, and are kept constant throughout this study, unless stated otherwise:

- absolute threshold on the norm of the residue for the Newton-Raphson corrector: $\epsilon_{\text{NR}} = 10^{-9}$ (the residue norm is checked at the end of each step, and correction is carried out only if necessary),
- ANM series threshold used for step length estimation: $\epsilon_{\text{ANM}} = 10^{-12}$,
- ANM series order: $N_{\text{series}} = 20$.

The choice of a small correction threshold ensures that the accuracy of a solution is mainly dependent on the accuracy of the discretization method, and not on that of the solver of the quadratic problem. Similarly, the choice of an even smaller ANM threshold ensures that the approximation at the end

[1] At least locally, and in the absence of bifurcation.

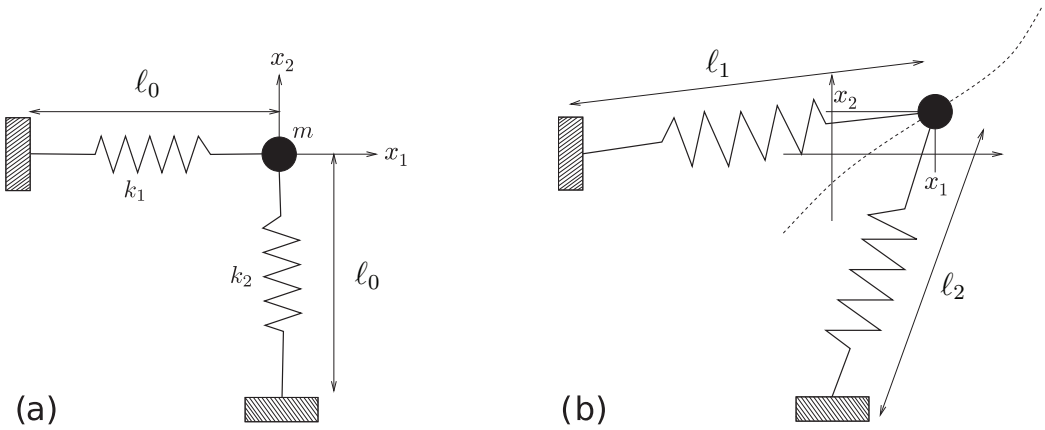

Figure 1: Sketch of the weakly nonlinear system: a mass m attached with two springs of strengths k_1 and k_2. **(a)** At rest the mass position is $(0, 0)$ and the springs are perpendicular with an identical length ℓ_0. **(b)** Taken away from its rest position, the mass position is noted (x_1, x_2) and the length of the springs are noted ℓ_1 and ℓ_2.

of each step is accurate enough so that no correction is usually needed at the beginning of the next step. Finally, the choice of the series order is arbitrary and mainly influences the step length.

3. Comparative study, case 1 : a weakly nonlinear system

3.1. A toy model with large displacements and geometrical nonlinearities

In this example, a point mass m is constrained by two perpendicular springs (at rest) of stiffness k_1 and k_2, each having a rest length ℓ_0 (see figure 1 for a sketch). The strain definition of Green-Lagrange is used, in order to account for large displacements, and the corresponding stress that is derived differs from the classical "$F = -ku$" law of springs. This model is representative of thin shells under large displacements, with geometrically induced nonlinearities. More details about the model are found in Arquier et al. [24].

Denoting $u_i = x_i/\ell_0$ the displacement of the mass in the plane, the i-th spring Green-Lagrange strain reads[2]:

$$e_i = \frac{1}{2}\frac{\ell_i^2 - \ell_0^2}{\ell_0^2} = u_i + \frac{1}{2}(u_1^2 + u_2^2) \tag{9}$$

From now on, the values $\ell_0 = 1$ and $m = 1$ are assumed, in a given system of units, as different values only result in a scaling of the problem.

Then, the equation of motion for the mass in direction x_i reads:

$$mu_i'' + N_i + u_i(N_1 + N_2) = 0 \tag{10}$$

where $N_i = k_i e_i$ is the stress in each spring.

The system's equations of motion then reads:

$$u_i'' = -N_i - u_i(N_1 + N_2). \tag{11}$$

3.2. Continuation parameter

When calculating a family of periodic solutions of such a system using numerical continuation, a crucial problem arises: no explicit parameter exists in the system equations (10). However, as Sepulchre and MacKay [25] showed, such conservative Hamiltonian systems do have periodic orbits belonging to 1D family whose implicit parameter is the total mechanical energy of the system (the first integral). Muñoz Almaraz et al. [26] proposed to add a small dissipative term to the equation proportional to, say, λ: a parameter that will vanish along the locus of periodic solutions.

Here, the resulting dissipative, perturbed system reads:

$$u_i'' = -N_i - u_i(N_1 + N_2) - \lambda u_i' \qquad i = 1, 2 \tag{12}$$

[2]Note that if the displacements were small, this definition could be linearized and would lead to the classical definition of the strain for a spring: $(\ell - \ell_0)/\ell_0$.

where λ is an explicit continuation parameter. This new system will have exactly the same periodic solutions as the original system if and only if $\lambda = 0$. Thus the standard continuation framework $\mathbf{R}(\mathbf{U}, \lambda) = 0$ can be used to compute the family of periodic solutions of this system.

3.3. First-order, quadratic form

Using additional variables, one can rewrite the system (12) as a set of quadratic first-order ordinary differential equations and algebraic equations as follows:

$$u_1' = v_1 \tag{13a}$$

$$u_2' = v_2 \tag{13b}$$

$$v_1' = -\lambda u_1' - N_1 - u_1(N_1 + N_2) \tag{13c}$$

$$v_2' = -\lambda u_2' - N_2 - u_2(N_1 + N_2) \tag{13d}$$

$$0 = N_1 - k_1 u_1 - \frac{1}{2} k_1 (u_1^2 + u_2^2) \tag{13e}$$

$$0 = N_2 - k_2 u_2 - \frac{1}{2} k_2 (u_1^2 + u_2^2) \tag{13f}$$

where (v_1, v_2) are the horizontal and vertical components of the mass velocity. The system thus has two degrees of freedom, which usually leads to only 4 state variables. However, because of the additional variables N_1 and N_2, the (augmented) state vector has size $n = 6$:

$$\mathbf{Y}(t) = [u_1(t), u_2(t), v_1(t), v_2(t), N_1(t), N_2(t)]^t.$$

In what follows, the following numerical values are used: $k_1 = 1$ and $k_2 = 2$ (in the chosen system of units).

3.4. Convergence study

The first family of periodic orbits is considered, that is locally tangent (at low amplitudes) to the first oscillator linear mode: $u_1'' = -u_1, \quad u_2 = 0$.

This family, or nonlinear normal mode, is implicitly parametrized by the total mechanical energy $E_m = \frac{1}{2}(m(v_1^2 + v_2^2) + k_1 e_1^2 + k_2 e_2^2)$. On this mode, the solution characterized by $E_m = 0.5$ is retained. To this end, a branch is computed for each discretization, and this solution point is located on the branch using a dichotomy algorithm up to a relative precision of $\epsilon_{Em} = 10^{-12}$ on the total mechanical energy.

To assess the convergence, the relative error (in the norm 2) between each of the solutions obtained with a given approximation (i.e. the solution with a given H value in the case of the HBM, and a given N value in the case of the collocation) and a reference solution is computed. This error is evaluated in the time domain by computing the time series of the solutions sampled at 2000 equidistant points over one period.

Denoting $\mathbf{Y}(t_i)$ the time series of the state vector of a given approximated solution (where t_i=$iT/2000$, i=1..2000) and $\mathbf{Y}_{\mathrm{ref}}(t_i)$ that of the reference solution, the chosen norm reads:

$$\epsilon_r = \frac{||[\mathbf{Y}(t_i) - \mathbf{Y}_{\mathrm{ref}}(t_i)]_{i=1..2000}||_2}{||[\mathbf{Y}_{\mathrm{ref}}(t_i)]_{i=1..2000}||_2} \tag{14}$$

In the present case, the system being perfectly smooth and weakly nonlinear, the Fourier series of any solution converges quickly, and the reference solution has been computed using HBM with $H = 128$ harmonics for which a very small residue norm has been achieved[3]: $||\mathbf{R}(\mathbf{U}_{ref})|| = 2.95 \times 10^{-16}$.

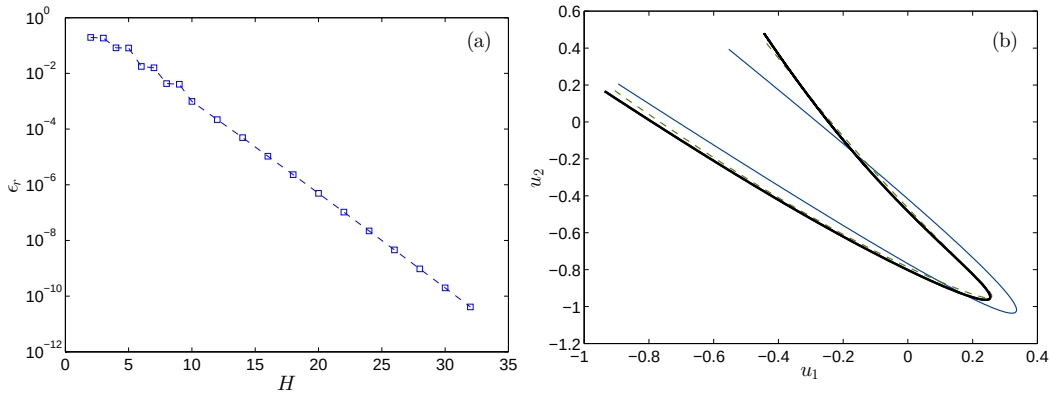

Figure 2: Convergence of HBM solutions for the weakly nonlinear system (13). The chosen solution, on each branch of periodic solutions has a total mechanical energy $E_m = 0.5$. **(a)** The norm-2 relative error ϵ_r as a function of the number of harmonics H, in semi-logarithmic scale. **(b)** Trajectories in the (u_1, u_2) plane, of the approximated solutions with H=2 (—, blue), 4 (– –, green), 6 (– · –, red), and 8 (· · ·, orange) as well as the reference solution (—, black). The last three trajectories are superimposed, illustrating the fast convergence.

3.4.1. Frequency domain approach: high-order harmonic balance

Figure 2 displays, in the left part (a), the evolution of the relative error ϵ_r of the approximation as a function of the number of harmonics H, in a semi-logarithmic scale. It shows the typical exponential convergence of spectral methods. The stairs-like shape of the curve at low H values suggests that odd harmonics have little influence on the error, which is explained by the fact that the chosen solution is of moderate amplitude, therefore the dominant nonlinearity of the system is quadratic.

The right part of figure 2 shows trajectories of several approximations as

[3]The authors have also confronted this reference solution by comparing it to the result of a time marching scheme that provides error control along the trajectory. Using an extremely fine tolerance criteria and starting from identical initial conditions (up to machine precision), both solutions are found to be almost identical, with a relative norm-2 difference of the order of 1×10^{-11}.

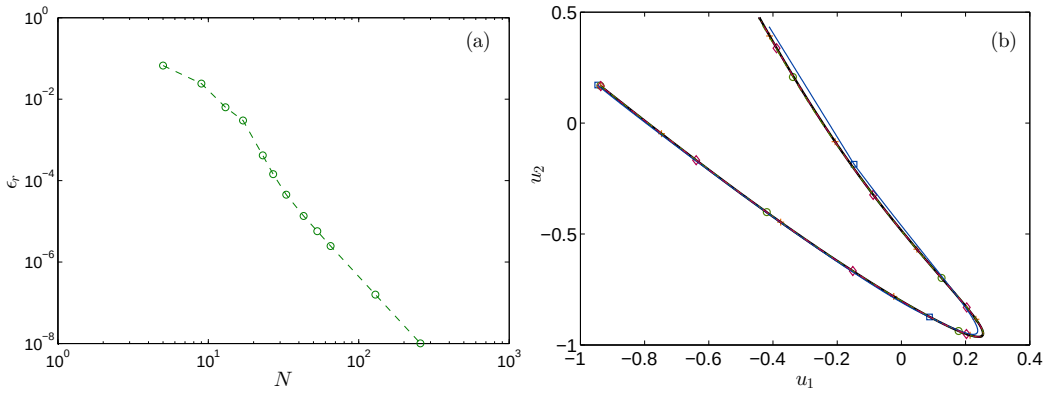

Figure 3: Convergence of orthogonal collocation with piecewise cubic polynomials on the weakly nonlinear system (13). The chosen solution, on the branch of periodic solutions has a total mechanical energy $E_m = 0.5$. **(a)** Norm-2 relative error ϵ_r as a function of the number of elements N, in logarithmic scale. **(b)** Phase diagram, in the (u_1, u_2) plane, of the approximated solutions with N=3 (—, squares, blue), 5 (– –, circles, green), 9 (– · –, diamonds, red), and 17 ($\cdots$, crosses, orange) as well as the reference solution (—, black). Markers indicate the location of the oscillator at t_j, the start of each of the N time interval subdividing the period. The last three curves are almost superimposed, illustrating the fast convergence.

well as of the reference solution in the (u_1, u_2) plane. The $H = 8$ solution thus is a very good approximation, both qualitatively (the trajectory is superimposed with that of the reference solution) and quantitatively ($\epsilon_r = 4.10^{-3}$).

3.4.2. Time domain approach: orthogonal collocation with piecewise cubic polynomials

Figure 3 displays, in the left part (a), the relative error of the approximation ϵ_r as a function of the number of elements (logarithmic scale). In the right part (b) of that figure, the shape of several approximations as well as that of the reference solution in the (u_1, u_2) plane are shown.

The semi-logarithmic error-plot (not displayed) shows an exponential convergence for $N < 27$ (first six points from the left end), whereas the logarithmic plot displayed here suggests an asymptotic convergence that is polyno-

mial in N (of order 4), for N sufficiently large. It is the expected asymptotic behavior, according to De Boor and Swartz [22], given that the system is perfectly smooth (the nonlinear terms are low order polynomials).

3.4.3. Comparison

In order to compare the two methods, the total number of equations involved in the final algebraic system needs to be taken into account. This number, denoted N_{tot}, is :

- $(2H+1)n+1$ in the case of the HBM,
- $(3N+1)n+1$ in the case of the collocation method.

Figure 4 clearly shows that, for this simple, smooth, weakly nonlinear system, HBM achieves a much quicker convergence. A fair comparison would require the use of a collocation with piecewise polynomials whose order p would be the refining parameter (with a fixed number of elements). However, for reasons explained above, it is beyond the scope of this study.

3.5. Computing a branch of periodic solutions

Figure 5 illustrates the branch of periodic solutions computed using HBM discretization (H=128 harmonics) and the ANM continuation. The mechanical energy along the horizontal direction $E_{m,1}=\frac{1}{2}mv_1^2+\frac{1}{2}k_1e_1^2$ and that along the vertical direction $E_{m,2}=\frac{1}{2}mv_2^2+\frac{1}{2}k_2e_2^2$ are plotted against the angular frequency ω. At low amplitudes (bottom-right corner), the nonlinear mode is tangent to the linear mode $(1,0)$.

Figure 6 illustrates the same branch in a classical frequency-energy plot. The branch obtained using HBM (H=128 harmonics) and that from collocation (N=85 elements, p=3 collocation points per element) are both plotted but are superimposed. Using the HBM with H=128 harmonics, the size

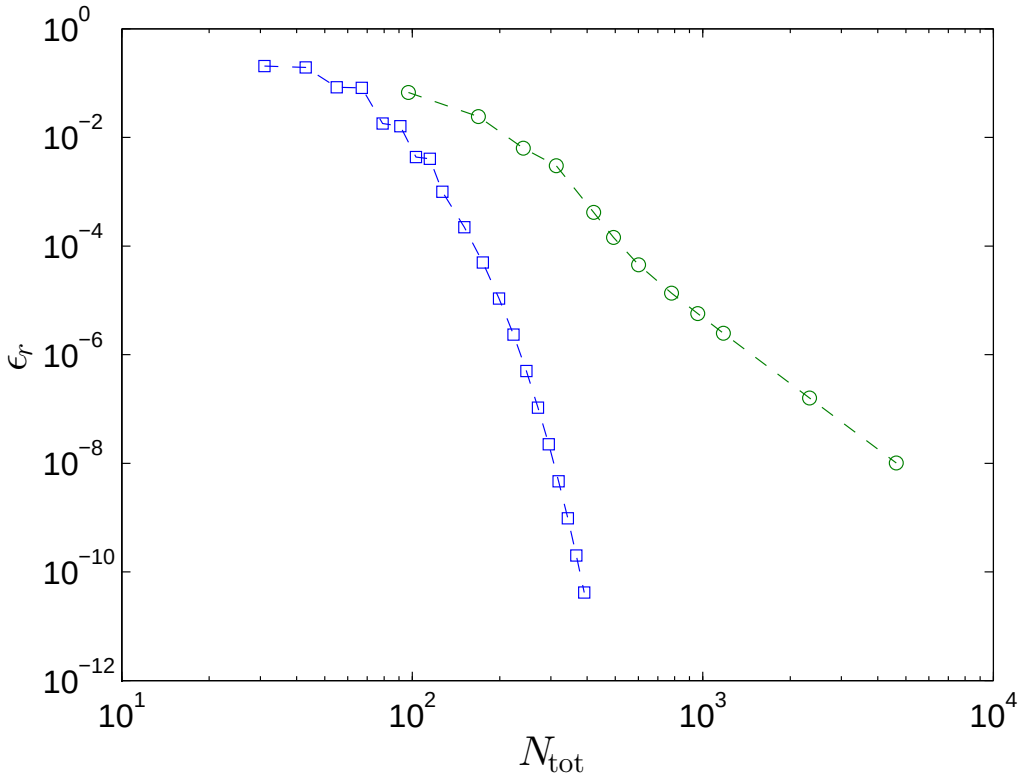

Figure 4: Norm-2 relative error (with respect to the reference solution) as a function of the total number of algebraic equations after discretization: comparison between HBM (squares, blue) and piecewise cubic polynomial collocation (circles, green).

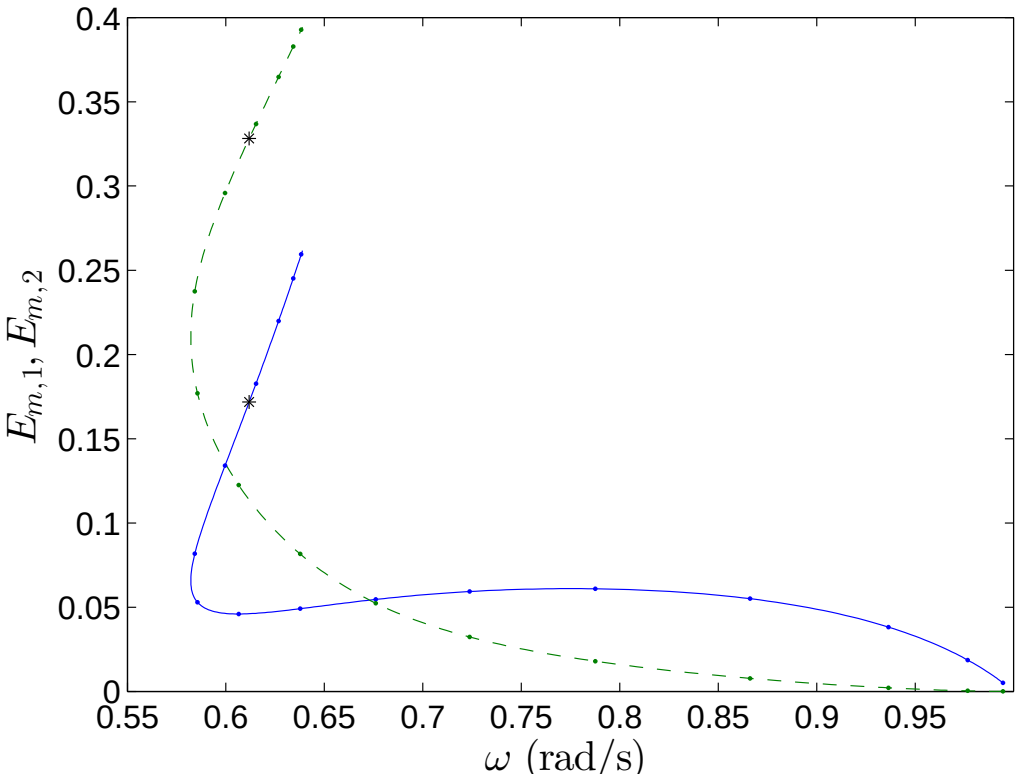

Figure 5: Branch of periodic solutions for the weakly nonlinear system (13) using HBM discretization and ANM continuation: mechanical energy of the system projected on the horizontal axis $E_{m,1}$ (—, blue) and on the vertical axis $E_{m,2}$ (– –, green) as functions of the angular frequency ω. Small dots indicate the continuation steps. The black star on each curve indicates the position of the solution used for the convergence study. Reference diagram computed using $H = 128$ harmonics.

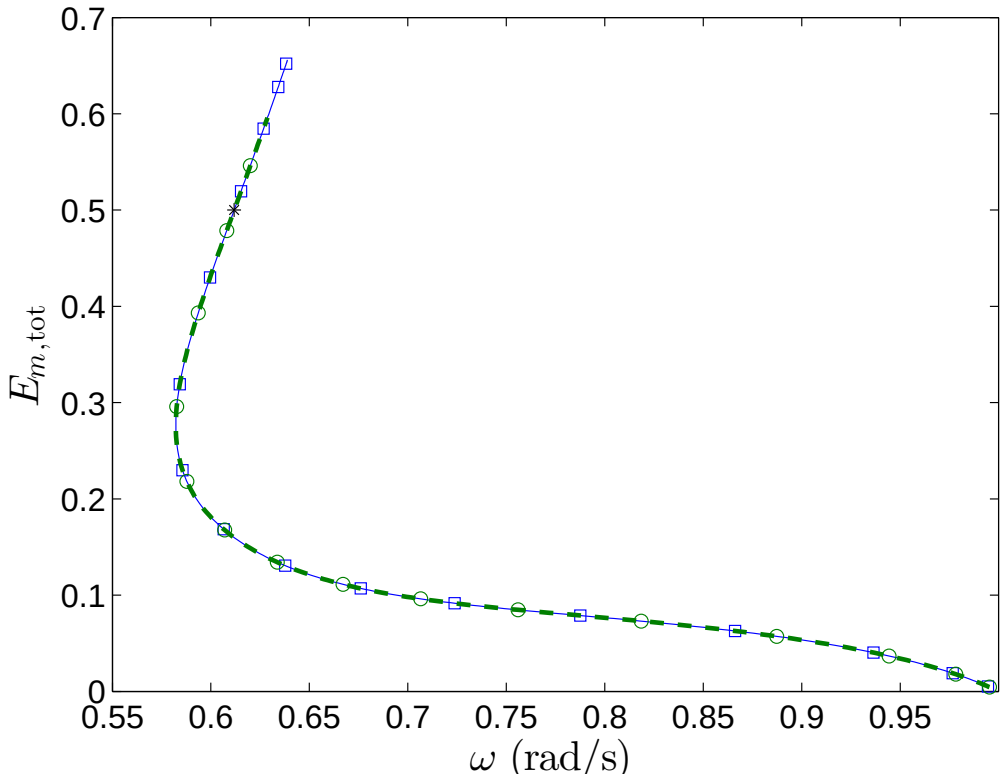

Figure 6: Branch of periodic solutions for the weakly nonlinear system (13): frequency-energy plot of the system obtained with HBM, H=128 harmonics (—, squares, blue) and collocation, N=85 cubic elements (− −, circles, green). The curves are superimposed. Blue squares indicate the continuation steps of the HBM branch, while green circles indicate that of the collocation branch. The black star indicates the position of the solution used for the convergence study.

of $\mathbf{R}(\mathbf{U})$ is N_{tot}=1543, and the target point where E_m=0.5 is reached after 12 continuation steps, starting from $u_1(0)$=−0.1 and ω=0.995rad/s. Using collocation with N=85 elements of order p=3, the resulting algebraic system size is N_{tot}=1537, and the target point with E_m=0.5 is reached after 14 continuation steps, from the same starting point.

To conclude the study of this weakly nonlinear system, HBM and collocation both appear to be efficient methods for computing the branch of periodic solutions with a numerical continuation tool. The HBM was found to show exponential convergence, while the collocation method showed polynomial convergence (with respect to N), as expected[4]. The next section will explore how these methods adapt to a very stiff nonlinearity.

4. Comparative study, case 2: a strongly nonlinear system

The same procedure is now applied to test both discretization methods on a stiff nonlinearity: an exponential function.

4.1. A simple oscillator impacting a rigid wall

This example consists in a one degree-of-freedom mass-spring like system, whose position is constrained in the half-plane $u < 1$ by a perfectly rigid wall, where $u(t)$ denotes the dimensionless position of the (unit) mass.

The wall reaction is regularized using an exponential function, with a coefficient α allowing for the tuning of the regularization stiffness:

$$F_r(u) = -\mathrm{e}^{\alpha(u-1)},$$

[4]Note that increasing the order p of the polynomials instead of the number of elements N would result in an exponential convergence as for the HBM.

The regularized impacting oscillator is governed by the following equation of motion:

$$u''(t) = -u(t) - \mathrm{e}^{\alpha(u(t)-1)}, \tag{15}$$

where the prime sign denotes time differentiation. Note that due to the form chosen for the wall reaction $F_r(u)$, the problem (15) is conservative. In what follows, the value $\alpha = 200$ is used, which corresponds to an extremely stiff regularization.

4.2. Continuation parameter

As for the first system, a dissipative perturbation is added to the system so that an explicit parameter λ appears in the equations, in order to use the classical framework $R(U, \lambda)$ for the continuation. The resulting system is now dissipative :

$$u''(t) = -u(t) - \lambda u'(t) - \mathrm{e}^{\alpha(u(t)-1)}, \tag{16}$$

where λ is the continuation parameter.

The perturbed system (16) has exactly the same periodic solutions as that of the conservative system (15) if and only if $\lambda = 0$.

For the treatment of the exponential nonlinearity in the quadratic framework of the ANM, the reader is referred to Karkar et al. [2] and Karkar [27]. The system is rewritten as follows:

$$u'(t) = v(t) \tag{17a}$$

$$v'(t) = -u(t) - \lambda v(t) - e(t) \tag{17b}$$

$$e'(t) = \alpha e(t) v(t) \tag{17c}$$

$$e(0) = \mathrm{e}^{\alpha(u(0)-1)} \tag{17d}$$

Thus, the number of ordinary differential equations is $n = 3$ (the last equation is only an initial condition and does not require any discretization), with the following state vector: $Y(t) = [u(t), v(t), e(t)]^t$.

4.3. Convergence study

The periodic solution corresponding to a total mechanical energy $E_m = \frac{1}{2}(1.5)^2 = 1.125$ is retained, ie. that with maximum amplitude reached during free flight of $||u||_{max} = 1.5$.

Given the stiffness of the nonlinearity, one needs to ensure that both methods converge to the "right" solution. Thus, a reference solution should be either analytically computed or numerically obtained through time integration with very coarse tolerance criteria.

4.3.1. Reference solution

Because the system is very stiff, one can expect the HBM to achieve much slower convergence than in the previous case. In the worst case, the convergence may not even be uniform. Thus, for this second example, an independent method, which allows error control, was chosen to construct a reference solution.

A time marching scheme especially designed for stiff systems is used. It is a single-step solver with adaptive step size, based on a modified Rosenbrock formula of order 2 (see [28]). On each component, the relative tolerance is set to 10^{-10} and the absolute tolerance to 10^{-12}.

The reference solution is computed from the starting point $(u, v) = (-1.5, 0)$, on a time interval long enough to get more than one period. The length of the period is then deduced by analysis of the computed orbit: an event is triggered when the orbit passes over the starting point and the instant of this event is recorded.

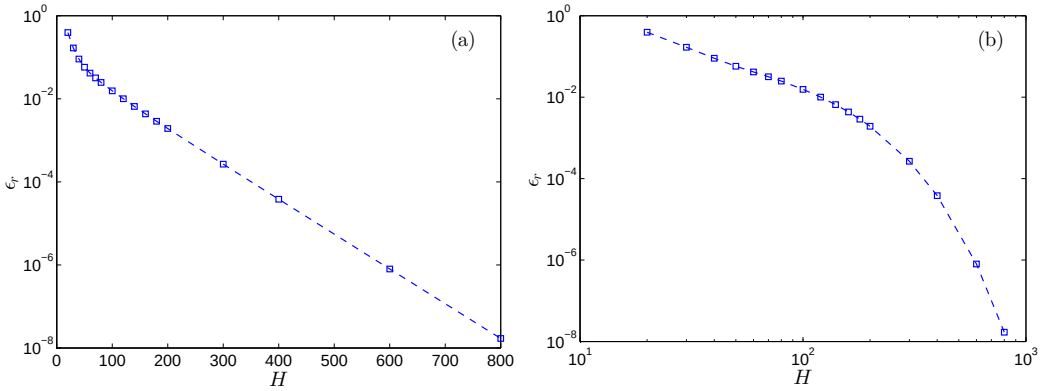

Figure 7: Convergence of the HBM for the strongly nonlinear system (17): a free, conservative impact oscillator regularized with a stiff (α=200) exponential. Norm-2 relative error ϵ_r with respect to the reference solution, as a function of the number of harmonics H retained in the approximation. **(a)** Semi-logarithmic scale. **(b)** Logarithmic scale. The solution is such that $||u||_{max}$=1.5.

4.3.2. Frequency domain approach : harmonic balance method

Figure 7 illustrates convergence of the HBM. The relative error ϵ_r with respect to the reference solution is plotted against the number of harmonics H retained in the approximation.

For each H value, the branch was followed by continuation until a sufficient amplitude was reached. Then, the solution point whose amplitude is such that $||u||_{max}$=1.5 was extracted from the branch by a dichotomy algorithm, with a relative precision of 1.10^{-12}.

For each value of H, a time series $[\mathbf{Y}(t_i)]$ was computed that consists in 2000 equally spaced samples over one period ($t_i = iT/2000,\ i = 1..2000$) and was compared to that of the reference solution $[\mathbf{Y}_{\text{ref}}(t_i)]$ by means of the relative error ϵ_r, as defined in the previous section (see equation (14)).

The convergence plot displayed figure 7, where ϵ_r is plotted against H, shows two distinct parts:

- first, for $H < 50$ (first four points), a polynomial convergence is ob-

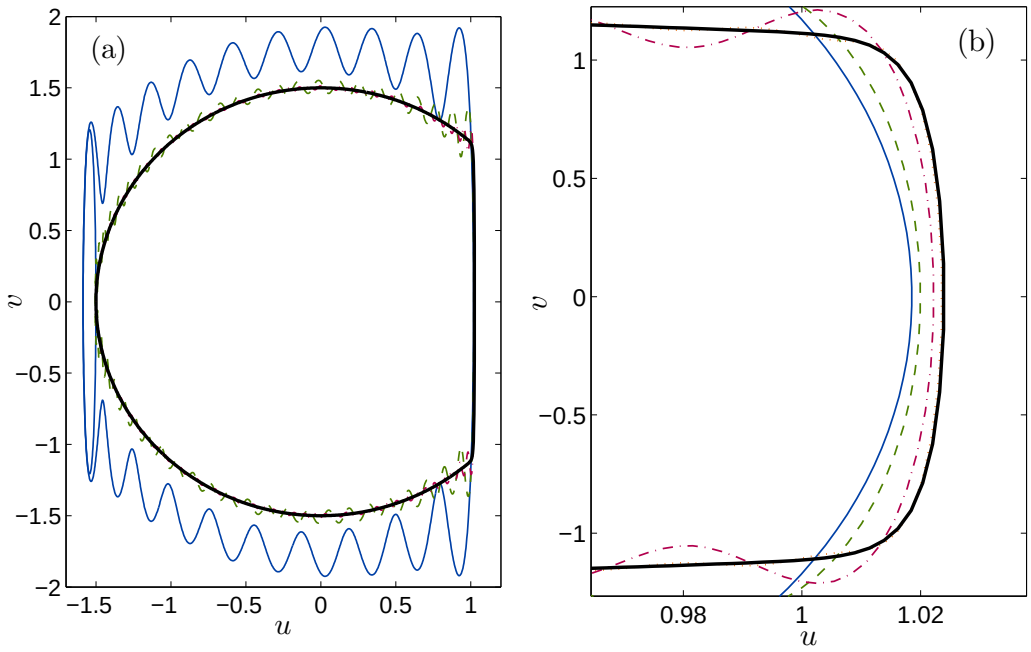

Figure 8: Phase diagram of the approximated solutions with H=20 (—, blue), 50 (– –, green), 100 (– · –, red), 200 (· · ·, orange), as well as the reference solution (▬, black). **(a)**: full scale diagram (the orange curve is not visible). **(b)**: zoom onto the impact zone (u=1), where all curves can be distinguished (orange and black almost superimposed).

served (straight line on a logarithmic scale), probably due to the fact that the approximation with such a low H value is not able to capture the sudden variations of trajectory during the impact;

- then, for $H > 50$, an exponential convergence is obtained (straight line on a semi-logarithmic scale), which is the expected asymptotic convergence of the HBM applied to a smooth system.

The phase diagram plotted on figure 8 is a perfect illustration of the observed phenomenon in the first convergence regime: the approximation is very crude with H=20, but tends quickly to the reference solution as H is increased, at least at the scale of the entire orbit. Refining the approximation with more than 100 harmonics only produces visible effects close to the stiff

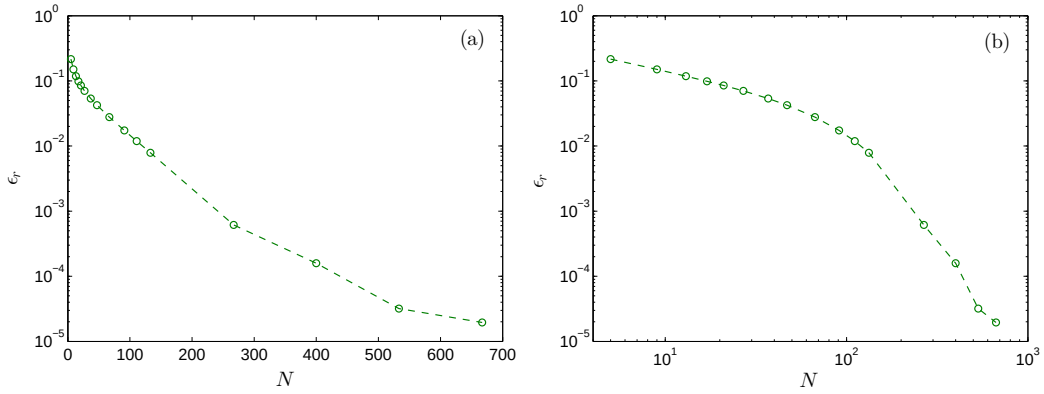

Figure 9: Convergence study of the collocation method for the strongly nonlinear system (17): a free, conservative impact oscillator regularized with a stiff (α=200) exponential. Chosen cycle amplitude: $||u||_{max}$=1.5. Norm-2, relative error with respect to a reference solution as a function of the number of elements N. **(a)** Semilogarithmic scale. **(b)** Logarithmic scale.

part of the orbit, near u=1, where the approximation with $H = 200$ can actually be distinguished from the reference solution. A slight penetration (approximately 2% of the total amplitude of the cycle) inside the "wall" is observed, as a result of the regularization. By tuning the α parameter, one can control this penetration, with respect to the cycle amplitude[5].

4.3.3. Time domain approach: orthogonal collocation with piecewise polynomials

The same analyses are now applied to the collocation method. The relative error is computed using the same definition as in the previous parts. Values of (u, v) at t_i are interpolated using cubic polynomials[6].

Figure 9 illustrates how the collocation method converges in three parts:

[5]One could also finely tune both the penetration and the stiffness of the system by using an additional multiplicative parameter in front of the exponential term.

[6]By definition, the elements used *are* cubic polynomials, written in the Lagrange basis defined on four equally spaced points, including borders. See section 2.

- first for $N \leq 27$, the relative error decreases polynomially (low order) in N: the first six points on the right plot (b), with a logarithmic scale, form a straight line;

- then for $27 \leq N \leq 267$, the convergence seems exponential in N: the corresponding points on the left plot (a), with a semi-logarithmic scale, form a straight line;

- finally for $N \geq 267$, the convergence seems polynomial (high order) in N.

In the last part of the figure, the points being not perfectly aligned suggest the asymptotic behavior is not yet reached.

In the case of a very smooth problem, Karniadakis and Sherwin [20] showed that it is more efficient to use higher degree interpolants than increasing the number of elements N. However, the "smoothness" of the problem is resolved after a minimal number of elements. Put differently, the stiffness of the system makes the transition (before reaching asymptotic convergence rates) longer. The low-order (~ 1) polynomial convergence is the result of the stiffness of the solution, and increasing the degree of the interpolants would probably not make the error decrease faster.

Thus, in the present case, increasing N is probably more efficient, at least up to N=267. Only after this point, where the high-order (~ 3) polynomial convergence is observed, may a p-refinement be preferable (for extremely high accuracy computations).

Figure 10 illustrates the phase diagram (u, v) of several approximations of the solution. Element boundaries are plotted using markers. Until N=67, one observes that the number of elements is too low to have at least one element inside the stiff part of the orbit (impact). For higher values of N,

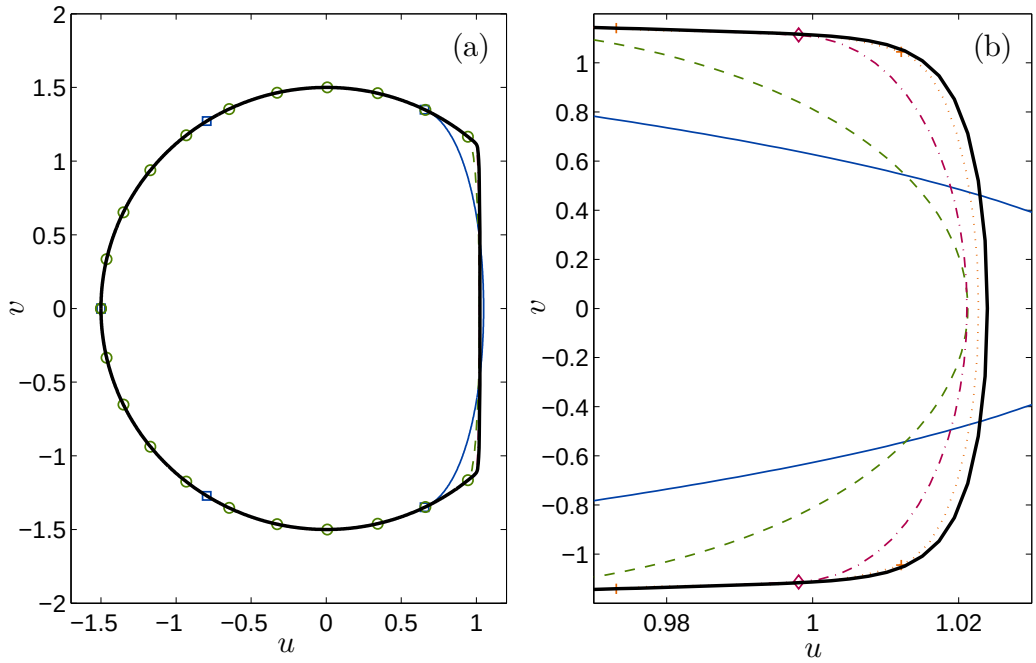

Figure 10: Phase diagram of approximated solutions using N=5 (—, squares, blue), 21 (– –, circles, green), 67 (– · –, diamonds, red), and 133 (· · ·, crosses, orange) as well as the reference solution (▬, black). **(a)** Full scale; markers show the element boundaries for the first two approximations (5 and 21 elements respectively). **(b)** Zoom onto the impact zone (u=1); markers (diamonds and crosses) indicate the element boundaries for approximations corresponding to 67 and 133 elements.

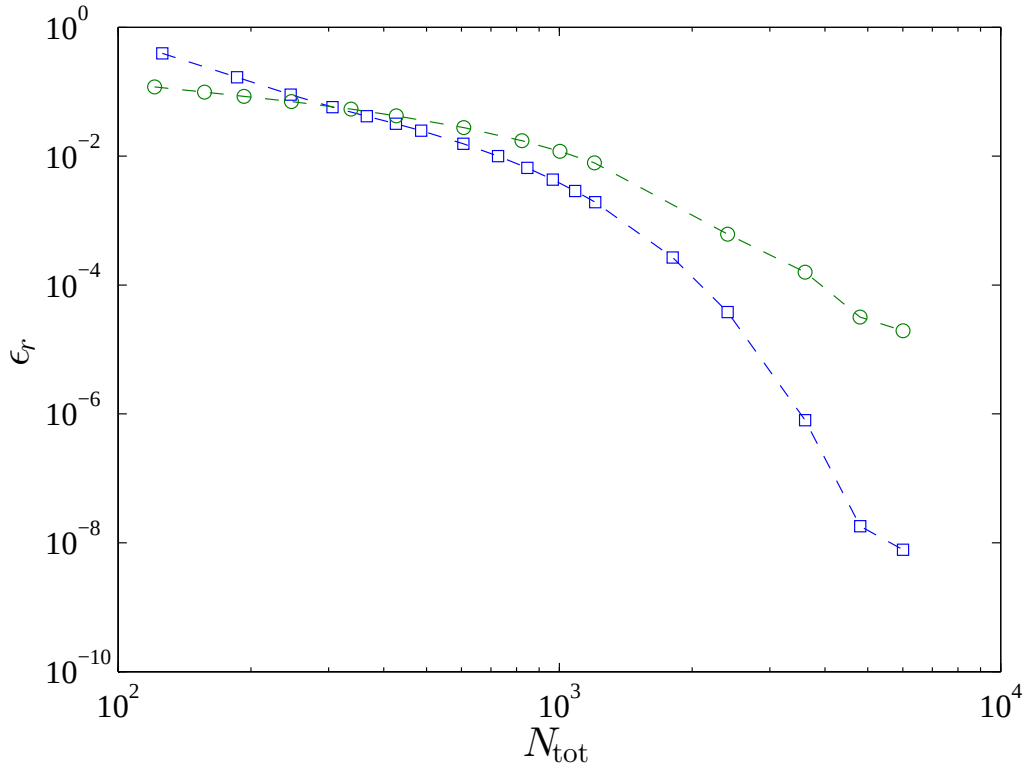

Figure 11: Comparison between harmonic balance (squares, blue) and collocation (circles, green): norm-2 relative error with respect to a reference solution as a function of the size of the final algebraic system (resulting from discretization). Case of the impacting oscillator regularized with a stiff exponential (α=200). Solution amplitude for the comparison: $||u||_{max}$=1.5.

element boundaries penetrate inside the stiff part of the orbit, allowing for a better representation of the solution as derivative discontinuities are possible at these points.

4.3.4. Comparison

Figure 11 shows the comparison of convergence curves for the two methods: $\epsilon_r = f(N_{\text{tot}})$, where the abscissa is the total size of the algebraic system resulting from the discretization:

- $N_{\text{tot}} = (2H + 1)n + 3$ for the HBM[7],
- and $N_{\text{tot}} = (3N + 1)n + 1$ for the collocation method.

Even though the approximation of the solution using a Fourier series with relatively few harmonics ($H < 50$) is relatively poor, the convergence rate gives the HBM an advantage. While the tangent matrix resulting from harmonic balance is less sparse and has a much greater bandwidth than that of a collocation method (thus, the computation time needed to compute this matrix and to invert it is longer, especially for very high H values), the convergence shows that for a given accuracy, a much smaller system is needed with the HBM than with the collocation.

Finally, given the limited resources of a classical PC workstation, the HBM allows for the computation of a much more precise solution compared to the collocation.

4.4. Continuation of periodic solutions

The branches of periodic solutions computed using both discretization techniques are shown in figure 12. Using ANM series up to order 20, and starting from the linear solution at $||u||_{max}$=0.9, it takes 26 steps to reach the point that corresponds to the solution ($||u||_{max}$=1.5) when using the HBM, while it takes 36 steps with the collocation method. The computation was carried out, in the first case, with H=1000 harmonics (N_{tot}=6006) and in the second case with N=667 (N_{tot}=6007). Both methods show a shortening of steps around the linear-nonlinear transition (expected result). However, the HBM leads to larger steps further down the branch, while the collocation leads to more or less constant (or even decreasing) step sizes.

[7]Note that there are two more variables than for the previous test case, because of additional variables e(0) and u(0) needed for the definition of initial condition 17d.

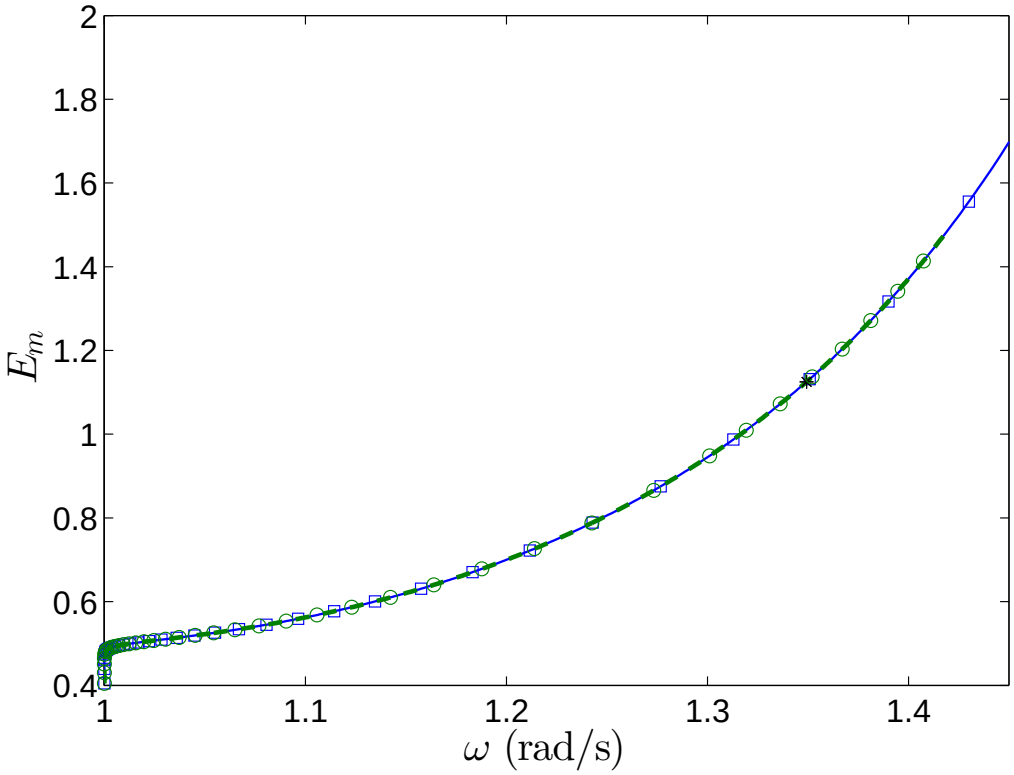

Figure 12: Frequency-energy plot of the branch of periodic solutions computed using HBM (—, squares, blue) and collocation (– –, circles, green) for the regularized impacting oscillator. Markers indicate the beginning of each continuation step. The star denotes the solution used in the convergence study. Fourier series order for the HBM: H=1000. Number of cubic elements for the collocation: N=667. Regularization parameter: α=200. All parameters of the ANM are identical to the previous example.

5. Conclusion

Two discretization methods for solving periodic boundary value problems were compared: the harmonic balance, which is based on the frequency domain, and the orthogonal collocation (at Gauss points) with piecewise polynomials, which is based on the time domain. The methods were compared to each other in terms of convergence, and as means to compute branch of periodic solutions using numerical continuation.

The main conclusion is that, in the absence of basis enrichment or adaptive harmonic selection (for the HBM), and without adaptive mesh or p-refinement (for the collocation), the harmonic balance method achieves better convergence rates, and thus allows for much more precise approximations, even in the case of very stiff systems. This is surprising since the spectrum is expected to be greatly enlarged by a stiff nonlinearity, and a time-based method could seem more appropriate to discretize such stiff solutions.

Of course, improvements exist for both methods. On the one hand, collocation methods have proved to be more efficient when using an adaptive mesh (the AUTO software [16] is a well known implementation). On the other hand, adaptive harmonic selection and basis enrichment are also known to improve drastically the convergence of the harmonic balance for non-smooth problems (see e.g. Kim and Perkins [12])

The lack of comparison in the literature is to be underlined, possibly due to the difficulty to apply the HBM at very high orders (here, up to 1000 harmonics) until recently. Further comparison using improved methods are needed.

Acknowledgment

This work was partially funded by the CNRS and the DGA, as well as the ANR project ADYNO. The authors also wish to thank Peter Redl for improving the language.

[1] B. Cochelin and C. Vergez. A high order purely frequency-based harmonic balance formulation for continuation of periodic solutions. *Journal of Sound and Vibration*, 324:243–262, 2009.

[2] S. Karkar, B. Cochelin, and C. Vergez. A high-order, purely frequency-based harmonic balance formulation for continuation of periodic solutions : the case pf non-polynomial nonlinearities. *Journal of Sound and Vibration*, 332:968–977, 2013.

[3] W. Szemplinska-Stupnicka. *The behaviour of nonlinear vibrating systems*. Kluwer academic publishers, 1990. ISBN 0-7923-0368-7.

[4] A. H. Nayfeh and B. Balachandran. *Applied Nonlinear Dynamics*. John Wiley and Sons, Inc., 1995. ISBN 0-471-59348-6.

[5] R. Seydel. *From equilibrium to Chaos*. Springer-Verlag, 1994. ISBN 0-387-94316-1.

[6] E. J. Doedel. Lecture notes on numerical analysis of nonlinear equations, 2010. URL `http://cmvl.cs.concordia.ca/auto/notes.pdf`. (last visited 06/01/2014).

[7] M. Urabe. Galerkin's procedure for nonlinear periodic systems. *Archive for Rational Mechanics and Analysis*, 20:120–152, 1965.

[8] T.M. Cameron and J.H. Griffin. An alternating frequency/time domain method for calculating the steady-state response of nonlinear systems. *Journal of Applied Mechanics*, 56(1):149–154, 1989.

[9] F. Thouverez, M. Guskov, and J.J. Sinou. Multi-dimensional harmonic balance applied to rotor dynamics. *Mechanics Research Communications*, 35:537–545, 2008.

[10] S.L. Lau and Y.K. Cheung. Amplitude incremental variational principle for nonlinear vibration of elastic systems. *Journal of Applied Mechanics*, 28:959–964, 1981.

[11] A. Grolet and F. Thouverez. On a new harmonic selection technique for harmonic balance method. *Mechanical Systems and Signal Processing*, 30:43–60, 2012.

[12] W.-J. Kim and N.C. Perkins. Harmonic balance/galerkin method for non-smooth dynamic systems. *Journal of Sound and Vibration*, 261(2): 213 – 224, 2003. ISSN 0022-460X. doi: 10.1016/S0022-460X(02)00949-5.

[13] A.M. Samoilenko and N. I. Ronto. *Numerical-analytic methods of investigating periodic solutions*. Mir Publisher, Moscow, 1979.

[14] L. Liu, E.H. Dowell, J.P. Thomas, P. Attar, and K.C. Hall. A comparison of classical and high-dimensional harmonic balance approach for a duffing oscillator. *Journal of Computational Physics*, 115:298 – 320, 2006.

[15] Hong-Hua Dai, Matt Schnoor, and Satya Alturi. A simple collocation scheme for obtaining the periodic solutions of the duffing equation, and

its equivalence to the high dimensional harmonic balance method: subharmonic oscillations. *Computer Modelling in Engineering and Sciences*, 84:459 – 497, 2012.

[16] E. J. Doedel and B. E. Oldeman. *AUTO-07P : Continuation and Bifurcation Software for Ordinary Differential Equations*. Concordia University, Montreal, Canada, January 2009. URL `http://cmvl.cs.concordia.ca/auto/`. (last visited 06/01/2014).

[17] W. Govaerts, Yu. A. Kuznetsov, V. De Witte, A. Dhooge, H.G.E. Meijer, W. Mestrom, A.M. Riet, and B. Sautois. *MATCONT and CL MATCONT: Continuation toolboxes in matlab*, 2013. URL `http://matcont.sourceforge.net/`. (last visited 06/01/2014).

[18] MATLAB. *version 7.7.0 (R2008b)*. The MathWorks Inc., Natick, Massachusetts, 2008.

[19] S. A. Orszag. Numerical Methods for the Simulation of Turbulence. *Physics of Fluids*, 12:250, January 1969. doi: 10.1063/1.1692445.

[20] G. E. Karniadakis and S. J. Sherwin. *Spectral/hp Element Methods For Computational Fluid Dynamics*. OXFORD University Press, 2005.

[21] D. Gottlieb and S. A. Orszag. *Numerical Analysis of Spectral Methods: Theory and Applications*. S.I.A.M., Philadelphia, Pennsylvania, 6th printing edition, 1977. ISBN 978-0-898710-23-6.

[22] C. De Boor and B. Swartz. Collocation at gaussian points. *SIAM J. Numer. Anal.*, 10(4), September 1973.

[23] S. Karkar, R. Arquier, B. Cochelin, C. Vergez, A. Lazarus, and

O. Thomas. *MANLAB 2.0, an interactive continuation software*, 2010. URL `http://manlab.lma.cnrs-mrs.fr`. (last visited 06/01/2014).

[24] R. Arquier, S. Bellizzi, R. Bouc, and B. Cochelin. Two methods for the computation of nonlinear modes of vibrating systems at large amplitudes. *Computer and Structures*, 84(24-25):1565 – 1576, 2006.

[25] J.-A. Sepulchre and R. S. MacKay. Localized oscillations in conservative or dissipative networks of weakly coupled autonomous oscillators. *Nonlinearity*, 10(3):679, 1997.

[26] F. J. Muñoz Almaraz, E. Freire, J. Galàn, E. Doedel, and A. Vanderbauwhede. Continuation of periodic orbits in conservative and hamiltonian systems. *Physica D: Nonlinear Phenomena*, 181(1-2):1 – 38, 2003. doi: 10.1016/S0167-2789(03)00097-6.

[27] Sami Karkar. *Numerical methods for nonlinear dynamical systems. Application to self-oscillating musical instruments.* PhD thesis, Aix-Marseille Univ., 2012. URL `http://tel.archives-ouvertes.fr/tel-00742651/`.

[28] L. F. Shampine and M. W. Reichelt. The matlab ode suite. *SIAM J. Sci. Comput.*, 18(1):1–22, January 1997.